

## Pure compressive solutions for masonry domes under gravity loads

Arsenio Cutolo<sup>1, a</sup>, Enrico Babilio<sup>1, b</sup>, Ida Mascolo<sup>1, c \*</sup> and Elio Sacco<sup>1, d</sup>

<sup>1</sup>Department of Structures for Engineering and Architecture (DiSt),  
University of Naples "Federico II", Naples, Italy

<sup>a</sup>arsenio.cutolo@unina.it, <sup>b</sup>enrico.babilio@unina.it, <sup>c</sup>ida.mascolo@unina.it, <sup>d</sup>elio.sacco@unina.it

**Keywords:** Dome, No-Tension Material, Membrane Equilibrium Problem, Thrust Surface Analysis, Finite Element Method

**Abstract.** In recent years, efforts have been made to compare equilibrium solutions of masonry domes obtained through different methods. The research summarized in the present paper focuses on the evaluation of the equilibrium of masonry domes in the context of the classical membrane theory, in comparison with more sophisticated finite element models. In particular, we consider solutions, with vanishing tensile stresses, for domes under gravity loads. The equilibrium problem is traced back to the equilibrium of a thrust surface under the assumption of no-tension material in the sense of Heyman (i.e., no tensile strength, infinite resistance in compression, and no slide along fracture lines). A finite difference discretization of the equilibrium equation is proposed and the obtained solution is compared with results from a nonlinear finite element analysis. The good agreement of the results shows that both finite difference and finite element approaches represent reasonable and reliable alternative tools.

### Introduction

Masonry domes, widely used in monumental buildings, are great works of architecture and engineering with a long history dating back to the dawn of civilization. Their static behavior has been widely studied through different methods which can be broadly classified into equilibrium methods [1–3] and deformation methods [4–6]. The present work aims at comparing equilibrium solutions for masonry domes under gravity loads obtained by applying a membrane approach and a Finite Element (FE) analysis. For the sake of comparison, we will consider very simple examples for which a reliable membrane solution can be easily obtained and then used to validate the more sophisticated FE results.

The paper is organized as follows. Section 2 presents the theoretical framework of the membrane approach and the Finite Difference (FD) algorithm used for the computations. Section 3 focuses on the fully three-dimensional, nonlinear FE analysis. Section 4 presents the findings of the two numerical-based analyses, remarking on the substantial agreement between the two approaches. This highlights the consistency and robustness of the nonlinear FE analysis for masonry domes characterized by very reduced tensile strength, as emphasized in the concluding remarks in Section 5.

### Membrane approach and FD solution

Let us consider a masonry dome subjected to its self-weight and assume its equilibrium may be written in agreement with Pucher's approach to the classical membrane theory [7-10]. We define an axial-symmetric (with respect to the direction of the load) membrane as an unknown function  $g = g(r)$ , where  $r$  is the radius of the membrane projection  $\Omega$  on the support plane, orthogonal to the direction of the load. The generalized stresses along the meridian and parallel curves on the membrane are  $S_{rr}$  and  $S_{\theta\theta}$ , respectively, and  $S_{11}$  and  $S_{22}$  are the corresponding projections on  $\Omega$ . By introducing an unknown Airy's stress function  $\varphi = \varphi(r)$  such that

$$\varphi' = \frac{r S_{rr}}{\sqrt{1+g'^2}} = r S_{11}, \quad \varphi'' = S_{\theta\theta} \sqrt{1+g'^2} = S_{22}, \quad (1)$$

the equilibrium along the direction of the load is given by the differential Pucher's equation

$$\varphi' g'' + \varphi'' g' = \gamma s r \sqrt{1+g'^2}, \quad (2)$$

where the prime symbol (') denotes the derivative with respect to the membrane radius  $r$ , and  $\gamma$  and  $s$  stand for the specific weight of the masonry and the thickness of the dome, respectively.

In the problem we are dealing with, the function  $g$  is admissible if it corresponds to a membrane fully contained within the dome thickness and the function  $\varphi$  is admissible if leads to non-positive stresses. Since in Eq. (2) both  $g$  and  $\varphi$  are unknowns, one can assign any tentative  $g_0$  or  $\varphi_0$  function and compute the other. Choosing  $n + 1$  not uniformly spaced points along the radius  $r$  on the platform  $\Omega$ , we transform Eq. (2) in a set of  $n + 1$  algebraic equations with  $2(n + 1)$  unknowns  $g(i)$  and  $\varphi(i)$ ,  $i = 0, 1, \dots, n$ . In a finite difference fashion, to compute the discrete derivatives of functions we are dealing with, we use three-point stencils and adopt central differences for any point  $1 \leq i \leq n$ , forward difference scheme for the point 0, backward difference scheme for the point  $n$ , thus making as simple as possible the setting of the boundary conditions.

To determine the solution to the discretized problem, a two-stage algorithm is implemented in *Mathematica*<sup>®</sup>, taking advantage of the possibilities of that high-level, general-purpose programming environment.

### Fully three-dimensional, nonlinear FE analysis

Modelling, simulations, and FE analysis are performed by means of the FE package Ansys<sup>®</sup>, adopting the concrete constitutive model (CCM) for masonry, which uses the William–Warnke constitutive equations [11] with a failure surface which is smooth and convex with noncircular and no affine sections in the deviatoric plane.

The performed analysis takes into account the geometric nonlinearities by means of an incremental approach based on a modified Newton-Raphson method [12-14]. An *ad hoc* algorithm is written in the Ansys Parametric Design Language (APDL) [15] to compute the coordinates of some points of the thrust surface on (any) vertical cross-section of the dome.

### Numerical results and method comparison

In the following numerical applications, we consider here a hemispherical dome with a mean radius of 12.5 m, a constant thickness of 2 m, and self-weight  $\gamma = 16 \text{ kN/m}^3$ .

#### Finite difference solution

The FD solution of Eq. (2) is summarized in Figures 1a and 1b reporting the computed function  $\varphi(r)$  and the stresses per unit length, respectively. We observe that at the end of the first stage of the FD algorithm, in the compressed part of the dome, the numerical solution is in agreement with the predictions of the classical theory of shells (dashed lines in Figure 1b), while at the end of the second stage, the generalized stresses tend to relax (see, in particular, the hoop stress and the horizontal thrust drawn, respectively, in red and black in Figure 1b).

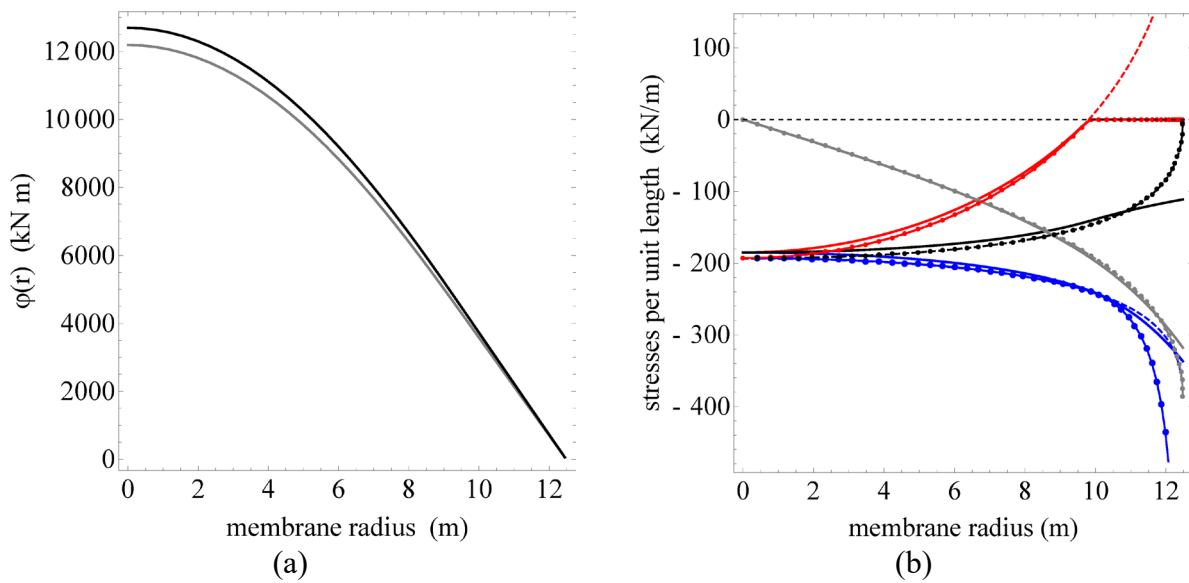


Figure 1: (a) Stress function  $\varphi(r)$ : FD solutions from the first (black) and second (gray) stages of the algorithm. (b) Generalized stresses  $S_{rr}$  (blue),  $S_{\theta\theta}$  (red), horizontal thrust  $S_{11}$  (black), vertical thrust  $S_v = S_{11} g'$  (gray), theoretical solution for hemispherical membrane (dashed lines): FD solutions from the first (dotted lines) and second (thick lines) stages of the algorithm

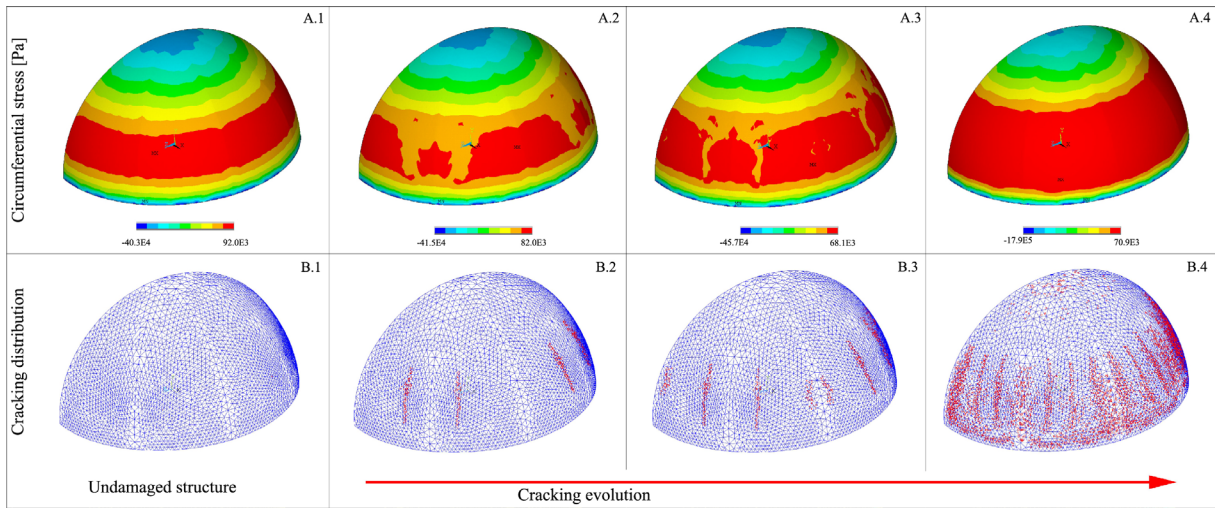
### Finite element solution

For the FE model, we consider a Cartesian reference frame  $(0, x_1, x_2, x_3)$ , with the origin  $O$  corresponding to the center of the projection of the dome onto the support plane  $x_2 = 0$ , being  $x_2$  the gravity direction. On account of the hemispherical symmetry of the analyzed problem, the computational effort in the analysis is reduced by considering only half of the dome, where  $x_1 = 0$  is the cutting plane. The dome is loaded only by gravity loads and mechanical parameters of masonry, namely Young's modulus, Poisson's ratio, and density, are set as  $E = 2\text{GPa}$ ,  $\nu = 0.1$ ,  $\rho = 1630.99\text{kg/m}^3$ . For the CCM, only the ultimate uniaxial tensile strength and the ultimate uniaxial compressive strength are assumed as failure parameters, set as  $\sigma_t = 1\text{MPa}$  and  $\sigma_c = -20\text{MPa}$ , respectively. Two models which differ in terms of boundary conditions are considered:

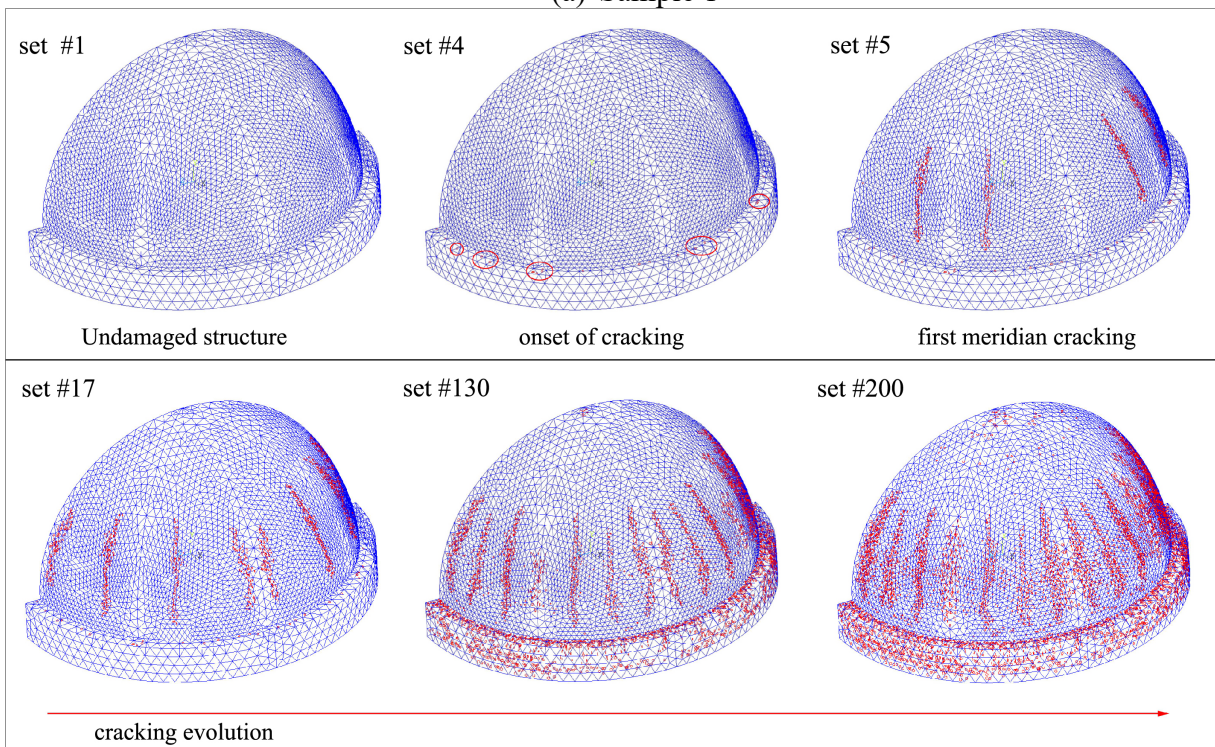
**Sample 1** discretized by means of 75,896 SOLID65 linear tetrahedral elements, resulting in 15,706 nodes with three translational degrees of freedom each, adopting the following boundary conditions are used in the simulations:

- displacements along the direction  $x_1$  are prevented, i.e.  $u_1 = 0$ , for all nodes which belong to the plane of equation  $x_1 = 0$ ;
- displacements along the radial direction, i.e. along the lines from the origin of the axes are allowed, for all nodes which belong to the plane of equation  $x_2 = 0$ ;
- displacements along the direction  $x_3$  are prevented, i.e.  $u_3 = 0$ , for all nodes which belong to the plane of equation  $x_3 = 0$ .

**Sample 2** discretized by means of 264,800 SOLID65 linear tetrahedral elements, resulting in 48,853 nodes with three translational degrees of freedom each. With the purpose of mimicking as accurately as possible the real boundary conditions of the dome, the drum is also partially modeled. The drum, 2.8 m high and 3.3 m wide, is fully-constrained at the base. Moreover, displacements along the horizontal direction  $x_1$  are prevented for all nodes which belong to the plane of equation  $x_1 = 0$ .



(a) Sample 1



(b) Sample 2

Figure 2: Nonlinear FE simulation of cracking

The nonlinear FE simulation of cracking for the *Sample 1* and *Sample 2* are reported in Figures 2a and 2b, respectively. We can observe that the two samples exhibit a fairly similar cracking evolution with the development of typical meridian cracks due to the masonry weakness to sustain hoop stresses. The cracking arises at the springing subsequently propagating vertically upwards toward the crown (*Sample 1* and *Sample 2*) and downwards into the drum (*Sample 2*) and arresting at the haunches, as expected [16]. Figure 3 reports a superimposition of the thrust surface cross-section obtained by means of the membrane approach and the two FE samples. We emphasize that the lines computed from FE solutions are in agreement with the thrust surface cross-section obtained with the membrane approach, by imposing the initial point of the thrust line at the crown of the dome and the final point at the springing of the dome coincident with the corresponding

points evaluated with FE simulations. We argue that the comparison shows the reliability of the performed FE analysis.

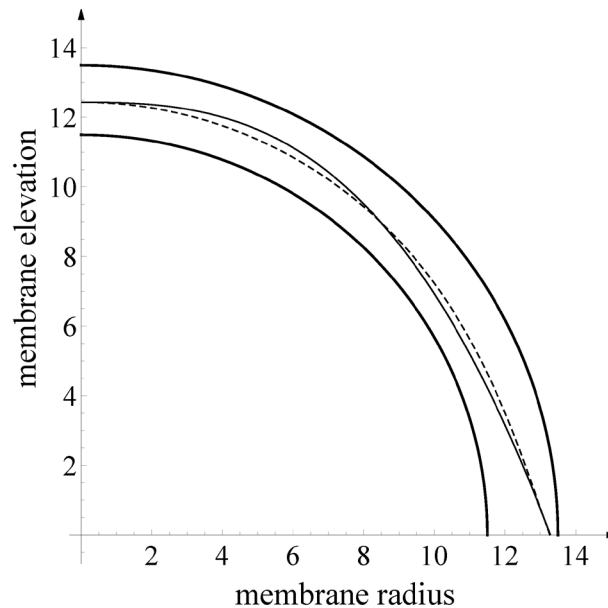


*Figure 3: Superposition of the thrust surface to the half cross-section of the dome: membrane approach (dashed line) vs. FE approach (solid black line)*

## Conclusions

In the present contribution, two thrust surfaces in the thickness of a simple hemispherical masonry dome, under its self-weight, are computed: one integrating the Pucher's equilibrium equation through a finite difference approach, the other obtained from a more sophisticated constitutive model accounting for damage and smeared crack implemented into a finite element model. The solution from the membrane Pucher's approach, applied to a very simple example, is here assumed as the benchmark to assess the FE results. However, while the membrane approach is flexible enough to solve a large class of problems, its FD discretization becomes cumbersome in the case of complex geometries. In such cases, finite element models are instead suitable. In this respect, the utility of a Pucher-based solution represents a simple and physically significant benchmark for the FE model characterized by a large number of parameters that need to be carefully set up. In fact, the agreement between the thrust surface cross-section obtained with the nonlinear elastic analysis and the membrane approach demonstrates the reliability and usefulness of the proposed FE approach.

## References

- [1] M. Como, Statics of historic masonry constructions: An essay, in *Masonry Structures: Between Mechanics and Architecture*. Springer, 2015, pp. 49–72. [https://doi.org/10.1007/978-3-319-13003-3\\_3](https://doi.org/10.1007/978-3-319-13003-3_3)
- [2] N. A. Nodargi and P. Bisegna, A new computational framework for the minimum thrust analysis of axisymmetric masonry domes, *Engineering Structures*, vol. 234, p. 111962, 2021. <https://doi.org/10.1016/j.engstruct.2021.111962>
- [3] A. M. D'Altri, V. Sarhosis, G. Milani, J. Rots, S. Cattari, S. Lagomarsino, E. Sacco, A. Tralli, G. Castellazzi, and S. de Miranda, Modeling strategies for the computational analysis of

- unreinforced masonry structures: review and classification, *Archives of Computational Methods in Engineering*, vol. 27, no. 4, pp. 1153–1185, 2020. <https://doi.org/10.1007/s11831-019-09351-x>
- [4] C. Olivieri, C. Cennamo, C. Cusano, A. Cutolo, A. Fortunato, and I. Mascolo, Masonry spiral stairs: A comparison between analytical and numerical approaches, *Applied Sciences*, vol. 12, no. 9, p. 4274, 2022. <https://doi.org/10.3390/app12094274>
- [5] N. A. Nodargi and P. Bisegna, A finite difference method for the static limit analysis of masonry domes under seismic loads, *Meccanica*, vol. 57, no. 1, pp. 121–141, 2022. <https://doi.org/10.1007/s11012-021-01414-3>
- [6] M. Angelillo, E. Babilio, and A. Fortunato, Singular stress fields for masonry-like vaults, *Continuum Mechanics and Thermodynamics*, vol. 25, no. 2-4, pp. 423–441, 2013. <https://doi.org/10.1007/s00161-012-0270-9>
- [7] M. Angelillo, E. Babilio, A. Fortunato, M. Lippiello, and A. Montanino, Equilibrium of masonry-like vaults treated as unilateral membranes: Where mathematics meets history, *Civil-Comp Proceedings*, vol. 108, 2015.
- [8] E. Babilio, C. Ceraldi, M. Lippiello, F. Portioli, and E. Sacco, Static analysis of a doublecap masonry dome, in *Proceedings of XXIV AIMETA Conference 2019*, A. Carcaterra, A. Paolone, and G. Graziani, Eds. Springer International Publishing, 2020, pp. 2082–2093. [https://doi.org/10.1007/978-3-030-41057-5\\_165](https://doi.org/10.1007/978-3-030-41057-5_165)
- [9] C. Olivieri, A. Castellano, I. Elia, A. Fortunato, and I. Mascolo, Horizontal force capacity of a hemi-spherical dome, in *8th International Conference on Computational Methods in Structural Dynamics and Earthquake Engineering, COMPDYN 2021*, 2021, pp. 614–625. <https://doi.org/10.7712/120121.8513.19613>
- [10] M. De Piano, M. Modano, G. Benzoni, V.P. Berardi, F. Fraternali, A numerical approach to the mechanical modeling of masonry vaults under seismic loading, *Ingegneria Sismica*, 34(4): 103–119, 2017.
- [11] K. J. Willam and E. P. Warnke, Constitutive model for the triaxial behaviour of concrete, *Proceedings of IABSE, International Association for Bridge and Structural Engineering*, vol. 19, pp. 1–30, 1975.
- [12] R. Shamass, G. Alfano, F. Guarracino, An Analytical Insight into the Buckling Paradox for Circular Cylindrical Shells under Axial and Lateral Loading, *Mathematical Problems in Engineering*, 2015, Article ID 514267. <https://doi.org/10.1155/2015/514267>
- [13] F. Guarracino, M.G. Simonelli, The torsional instability of a cruciform column in the plastic range: Analysis of an old conundrum, *Thin-Walled Structures*, 113: 273–286, 2017. <https://doi.org/10.1016/j.tws.2016.11.007>
- [14] I. Mascolo, M. Fulgione, M. Pasquino, Lateral torsional buckling of compressed open thin walled beams: Experimental confirmations, *International Journal of Masonry Research and Innovation*, 4(1-2), 150–158, 2019. <https://doi.org/10.1504/IJMRI.2019.096829>
- [15] M. K. Thompson and J. M. Thompson, *ANSYS mechanical APDL for finite element analysis*. Butterworth-Heinemann, 2017.
- [16] Z. Nanhai and Y. Jihong, Structural vulnerability of a single-layer dome based on its form, *Journal of Engineering Mechanics*, vol. 140, no. 1, pp. 112–127, 2014. [https://doi.org/10.1061/\(ASCE\)EM.1943-7889.0000636](https://doi.org/10.1061/(ASCE)EM.1943-7889.0000636)